

AD A094887

LEVEL

②

AD

CARRIER LOCALISATION IN INVERSION LAYERS
AND IMPURITY BANDS

ANNUAL TECHNICAL REPORT

by

M. PEPPER

November 1980

DTIC
SELECTED
FEB 11 1981
S C

EUROPEAN RESEARCH OFFICE

United States Army

London England

GRANT NUMBER DA-ERO - 78-G-098

GR: Cavendish Laboratory
Department of Physics
University of Cambridge
Cambridge
CB3 0HE
U.K.

1
2
3
4
5
6
7
8
9
0

Approved for Public Release;

distribution unlimited

81 2 00 120

UNCLASSIFIED

SECURITY CLASSIFICATION OF THIS PAGE (When Data Entered)

R&D 2596-EE

REPORT DOCUMENTATION PAGE		READ INSTRUCTIONS BEFORE COMPLETING FORM
1. REPORT NUMBER	2. GOVT ACCESSION NO.	3. RECIPIENT'S CATALOG NUMBER
	AD-A094887	
4. TITLE (and Subtitle) Carrier Localisation in Inversion Layers and Impurity Bands.		5. TYPE OF REPORT & PERIOD COVERED Annual Technical Report, Sep 79 - Nov 80
7. AUTHOR(s) M. Pepper		6. PERFORMING ORG. REPORT NUMBER DA-ERO-78-G-098
9. PERFORMING ORGANIZATION NAME AND ADDRESS Cavendish Laboratory, Dept. of Physics University of Cambridge, Cambridge CB3 0HE		10. PROGRAM ELEMENT, PROJECT, TASK AREA & WORK UNIT NUMBERS 1E 1T161102BH57-03
11. CONTROLLING OFFICE NAME AND ADDRESS USARDSG-UK Box 65, FPO NY 09510		12. REPORT DATE November 1980
14. MONITORING AGENCY NAME & ADDRESS (if different from Controlling Office)		13. NUMBER OF PAGES 28
16. DISTRIBUTION STATEMENT (of this Report)		15. SECURITY CLASS. (of this report) Unclassified
17. DISTRIBUTION STATEMENT (of the abstract entered in Block 20, if different from Report)		15a. DECLASSIFICATION/DOWNGRADING SCHEDULE DTIC ELECTED FEB 11 1981
18. SUPPLEMENTARY NOTES		
19. KEY WORDS (Continue on reverse side if necessary and identify by block number) (U) Silicon (U) Ballistic Injection (U) Silicon - Silicon Dioxide Interface (U) Low Temperatures (U) Phonons (U) Localisation		
20. ABSTRACT (Continue on reverse side if necessary and identify by block number) This report contains results on the ballistic injection of electrons between Al and n+ Si and Al and the Si inversion layer. This was the first experiment on ballistic injection between a semiconductor and a metal, and yielded results of considerably greater clarity than those found from the all metal work. Basically the phonons responsible for intervalley scattering can be clearly observed and the technique offers a means of		

076550

UNCLASSIFIED

SECURITY CLASSIFICATION OF THIS PAGE (When Data Entered)

20. Contd.

identifying the various subbands in the Si inversion layer. Plasmons could be observed and in future it is planned to extend this technique to III-V semiconductors.

The other area of research described in this report is a collaborative experiment with Dr. K. von Klitzing and Dr. G. Dorda. It is shown that the Hall resistance of a MOSFET, when the conduction band is quantized by a strong magnetic field, is related simply to the fine structure constant. The experiment is described in detail.

UNCLASSIFIED

SECURITY CLASSIFICATION OF THIS PAGE (When Data Entered)

ABSTRACT

This report contains results on the ballistic injection of electrons between Al and n+ Si and Al and the Si inversion layer. This was the first experiment on ballistic injection between a semiconductor and a metal, and yielded results of considerably greater clarity than those found from the all metal work. Basically the phonons responsible for intervalley scattering can be clearly observed and the technique offers a means of identifying the various subbands in the Si inversion layer. Plasmons could be observed and in future it is planned to extend this technique to III-V semiconductors.

The other area of research described in this report is a collaborative experiment with Dr. K. von Klitzing and Dr. G. Dorda. It is shown that the Hall resistance of a MOSFET, when the conduction band is quantized by a strong magnetic field, is related simply to the fine structure constant. The experiment is described in detail.

Accession For	NTIS GRA&I	<input checked="" type="checkbox"/>
DTIC TAB	<input type="checkbox"/>	<input type="checkbox"/>
Unannounced	<input type="checkbox"/>	<input type="checkbox"/>
Justification	<input type="checkbox"/>	
By	<hr/>	
Distribution/	<hr/>	
Availability Codes	<hr/>	
Dist	Avail Codes	<hr/>
Special		

A

KEYWORDS

Silicon

Silicon - Silicon Dioxide Interface

Phonons

Localization

Ballistic Injection

Low Temperatures

CONTENTS

1. Ballistic injection of electrons in metal-semiconductor junctions
 - 1a Phonon spectroscopy and impurity enhanced inelastic scattering in n^+ silicon
 - 1b Phonon spectroscopy of aluminium
 - 1c Phonon and subband spectroscopy of silicon inversion layers
2. A new method for high accuracy determination of the fine structure constant based on quantized Hall resistance

1. Ballistic injection of electrons in metal-semiconductor junctions

1a Phonon spectroscopy and impurity enhanced inelastic scattering in n⁺ silicon

It has been known for some time that the electron-phonon coupling in metals can be investigated by the use of point contacts. If the contact area is sufficiently small, structure is found in the I-V characteristic. Work by Yansen^{1,2} and Jansen et al.^{3,4} showed that $\frac{d^2 I}{dV^2}$ was proportional to the electron-phonon coupling constant, $g(\omega)$, given by

$$g(\omega) = \alpha^2(\omega) F(\omega). \quad (1)$$

Here $\alpha^2(\omega)$ is the square of the matrix element for electron-phonon coupling averaged over the Fermi surface, and $F(\omega)$ is the phonon density of states. These authors have investigated $g(\omega)$ for a number of metals.

The theory of electrical resistance arising from small contact areas was first considered by Maxwell⁵, who predicted a resistance R given by $1/2\sigma b$, σ is the bulk conductivity and b is the contact radius. Sharvin⁶ considered the ballistic nature of current flow which occurs when the contact radius is smaller than the bulk mean free path, ℓ . He derived the contact resistance, R , in the following manner. The current flowing through the junction, I , is given by

$$I = n e \sigma b^2 \delta v.$$

n is the carrier concentration and δv is the velocity acquired by a carrier on passing through the junction. If the Fermi energy, $E_F \gg eV$, v is given by $eV/2mv_F$, where V is the applied voltage and v_F is the Fermi velocity. Thus, $R = 2mv_F/ne^2\pi b^2 = 2\ell/\pi\sigma b^2$.

Wexler has given an interpolation formula,

$$R = \frac{(K)}{2\sigma b} + \frac{4K}{3\pi\sigma b}. \quad (2)$$

Here (K) is a function of the Knudsen ratio, ℓ/b , being 1 for $K = 0$ and ~ 0.7 for high K . The first term in equation 2 is a "Maxwell" term and the second a "ballistic" term, i.e. independent of the bulk mean free path. Theoretical work, for example van Gelder⁷, has shown that minima in $d^2 I/dV^2$ are due to electrons which are initially emitted but then scattered back into the contact region. Each minima corresponds to the onset of a particular scattering process. Van Gelder finds that

$$\frac{d^2 I}{dV^2} = \frac{5.3 e D T b}{\hbar v_F} g(eV). \quad (3)$$

Here e and \hbar have their usual meanings, D is a factor close to 1 for high emission number and T , which is near unity, is the transmission factor of the contact. It was found that the background in $d^2 I/dV^2$ arises from multiple phonon emission processes. All the previous work

on this topic utilized metal-metal junctions, and, in general, the principal peaks in the phonon density of states corresponded to minima in $d^2 I/dV^2$. In this work the first results were obtained on ballistic emission between a metal point contact (Al) and a degenerate semiconductor (Si). As will be shown the various phonon scattering processes are observed more clearly than for emission in metal-metal junctions.

The structures used comprised a thin film of Al , of thickness about 1 μm , separated from an n^+ diffusion in Si by a 500 \AA - 1000 \AA thick thermally grown film of SiO_2 . A filamentary contact, ("short"), between Al and the n^+ Si was formed by the application of a high field. For values of applied voltage up to 100 mV, the 4.2 K contact resistance was between 5 $k\Omega$ and 10 $k\Omega$ decreasing slightly with increasing voltage.

An important difference between this system and the metal-metal system is that there is here a considerable disparity between the conductivity of the Al and the conductivity of the n^+ Si of doping $1-3 \times 10^{20} \text{ cm}^{-3}$. This will result in the voltage drop occurring in the Si. Although the Al filament is probably polycrystalline the resistance of the filament was estimated to be small compared to the observed resistance. From equation 2 the radii of the contacts used in this work were estimated to be in the range 20 \AA - 50 \AA . It was possible to observe a small hole in the Al on the surface of the oxide where the filament had formed. This was about 1 μm in diameter, indicating that the filament narrows rapidly, or that the radius of contact is only a fraction of the total radius.

It is to be noted that this type of experiment is only possible in the absence of tunnelling, i.e. a depletion region is not present at the contact. This implies the use of n^+ doping and junctions with very small barrier heights. Unfortunately, it does not seem possible to use equation 1 for the extraction of the coupling constant $g(\omega)$. This is because most results are obtained for values of V where $eV \gtrsim E_F$, E_F being 200 meV for the n^+ Si used in this work. Even where $eV \gg E_F$, I does not increase as $V^{1/2}$, but faster than V , indicating that, perhaps, space charge effects are important in the depleted Si around the junction region.

Figure 1 shows $d^2 I/dV^2$ plotted against \sqrt{V} for injection into arsenic doped Si at 4.2 K, this is achieved by biasing the Si positive with respect to the Al . The major peaks are identified in the figure. Essentially, the strongest effects are associated with the T.A. phonon responsible for g scattering, i.e. between valleys on the same (100) axis, the g T.O. and, or, intravalley phonons. The low energy g process is forbidden in zero order by group theory and occurs as a higher order process⁸. It is to be stressed that the combination minima do not correspond to the simultaneous emission of phonons, as here we would expect the strength of the minima to decrease rapidly with increasing number of phonons emitted. Rather they are due to electrons which have emitted n phonons, where $n = 0, 1, 2 \dots$, over a period of time then emitting another and being scattered back into the junction.

Figure 2 shows the corresponding result for injection into phosphorus doped Si. The principal points are the reduction in strength of the lowest energy g process, the virtual disappearance of the major peak at 30.5 meV, and the appearance of new structure near 40 meV. Table 1 contains a summary of the results and compares them with those obtained from magneto-phonon resonance studies on high purity Si (Eaves et al.⁹).

From a qualitative point of view, it is reasonable that the heaviest impurity, As, enhances the lower energy modes. It is relevant that impurity resonances have been observed in infra-red absorption at 54.6 meV, (P), and 45.3 meV(As)¹¹, far from the structure reported here. The theory of absorption has been discussed by Dawber and Elliott¹¹, and their predicted optical resonances are also distant from the impurity aided scattering processes found in this work.

We propose the following explanation of the additional structure due to impurities. The new phonons which assist intervalley transitions are those found at the K point, (0.75, 0.75, 0), on the phonon dispersion curve¹². The scattering is an f process, i.e. between (100) and (010) valleys, and conservation of momentum is maintained by the electron transferring momentum to the impurity, which eventually emits a shower of low energy phonons. In addition, the presence of charged impurities will enhance the electron-phonon coupling. The As peak at 30.5 meV is associated with the TA phonon at K possessing Σ_3 symmetry. The Σ_4 phonon is not observed, being forbidden by time reversal symmetry. The transfer of momentum to the As likewise enhances the role of the g T.A. phonon which is normally weak. Phosphorus enhances the higher energy phonons near 40 meV, we associate these with the I.A. phonon at K with Σ_1 symmetry and the LO phonon at K with Σ_3 symmetry. Both these phonons are near 46 meV for pure Si, and possibly the shift in energy arises from a change in the force constants as well as the difference in mass between P and Si.

These differences between P and As were general but the strength of the modes, and the shape of the background, could differ between specimens prepared in different ways, with different values of doping. Figure 3 shows a case of injection into Si:P where $d^2 I/dV^2$ becomes negative; this appeared due to both strong Phosphorus enhancement and strong f scattering near 50 meV. This junction also showed evidence of oscillations, possible due to quantum effects, (when the modulation voltage was low), previously observed in metal-metal contacts (Jansen et al.¹⁴). It is not clear if these are due to interference effects between multiple junctions or diffraction effects in single junction injection.

The principle features of the phonon spectrum were apparent at 77K, as shown for Si:As in Figure 4. It is noteworthy that the 30.5 meV minimum is not as dominant at this temperature, possibly absorption processes arising from the enhanced density of low energy phonons increase the importance of conventional intervalley scattering.

Pronounced structure was observed at high energies and is reproduced in Figure 5. This structure consists of a double resonance, each resonance is sharp and the two are separated by ~8 meV. The change in $d^2 I/dV^2$ is, approximately, a factor of 30 greater than the change due to optical phonon coupling. The resonance is unlike the minima observed for phonon interactions, and indicates, that strong coupling is producing two minima in the electronic density of states. The energy and carrier concentration strongly suggest that the structure is due to a pair of plasmons, although the uncertainty in the carrier concentration prevents identification as a surface or bulk plasmon.

The maximum change in momentum of the electron gas is too small to allow plasmon enhanced intervalley scattering. Thus, this cannot be the origin of the splitting. This may result from valley-valley

interactions introducing a small, extra, anisotropy of the mass, or possibly, the effects of strain on surface plasmons. This point is being investigated in detail.

REFERENCES

- 1 Yansen, I.K., 1974 Soviet Phys. J.E.T.P., 39, 506
- 2 Yansen, I.K., 1977 Soviet J. Low Temp. Phys., 3, 726
- 3 Jansen, A.G.M., Mueller, F.M., Wyder, P., 1977 Phys. Rev. B, 16, 1325
- 4 Jansen, A.G.M., Mueller, F.M., Wyder, P., 1978 Science, 199, 1037
- 5 Maxwell, J.C., 1904 A Treatise on Electricity and Magnetism, Clarendon Press, Oxford
- 6 Sharvin, Yu.V., 1965 Soviet Phys. J.E.T.P., 48, 984
- 7 Van Gelder, A.P., 1978 Solid State Comm., 25, 1097
- 8 Ferry, D.K., 1976 Phys. Rev. B, 14, 1605
- 9 Eaves, L., Hoult, R.A., Stradling, R.A., Tidey, R.J., Portal, J.C. and Askenasy, S., 1975 J. Phys. C, 8, 1034
- 10 Angress, J.F., Goodwin, A.R. and Smith, S.D., 1968 Proc. Roy. Soc., A308, 111
- 11 Dawber, P.D. and Elliott, R.J., 1963 Proc. Phys. Soc., 81, 453
- 12 Weber, W., 1977 Phys. Rev. B, 15, 4789

FIGURE CAPTIONS

1. $d^2 I/dV^2$ for electron injection into Si:As at 4.2 K. The principal phonons are indicated. The g(T.O.) and intravalley (I.V.) phonons are too close in energy to be separated.
2. $d^2 I/dV^2$ for electron injection into Si:P at 4.2 K.
3. $d^2 I/dV^2$ for electron injection into Si:P at 4.2 K. The top curve showing possible quantum effects was obtained with a modulation voltage of 0.1 mV, the lower curve with 1 mV. The L and T $\Delta\ell$ phonons are clear, these are discussed in the following paper.
4. $d^2 I/dV^2$ for injection into Si:As at 77 K. The $\Delta\ell$ L phonon is clear as is the combination of this with the Q phonon. These are discussed in the following paper.
5. Structure in $d^2 I/dV^2$ attributed to two plasmons. The magnitude of the structure is about a factor of thirty greater than the strongest phonon produced minimum.

TABLE I

PRINCIPAL THERMAGNETIC SCATTERING PROCESSES IN Si.

Si:2P Energy of phonon ± 0.50 mev	Si:AS Energy of phonon ± 0.20 mev	High Parity Si, Obtained from Magneto-phonon Resonance by Eaves et al. (1975) $\pm 3\%$	Comments
9.3 12.3 15.3	9.4 10.5 11.9	12.25	g phonon, T.A. mode, which is forbidden by group theory. From the phonon dispersion curve the energy should be 12.7 mev, assuming the conduction band minimum to be at (0.63, 0, 0). The conductivity is much higher in Si and Si:2P has strong Si:Si.
17.3 22.4	17.3 18.8 20.3	19.3 18.8 20.3	g, L.A. mode, strong in Si:2P f, broadened to a higher energy in Si:2P. Lost in the strong as enhanced excitation in Si:AS.
31.5	30.5	30.5	This is small in Si:P, very strong in Si:AS. The suggested origin, described in the text, is an acoustic phonon at the K point with \mathbf{E}_3 symmetry.
33.3 42.5	Suggested origins are the \mathbf{E}_1 acoustic and \mathbf{E}_3 optical modes at K. These phonons are absent in Si:AS.

TABLE I contd.

Si:P Energy of Phonon ± .05 mev	Si:As Energy of Phonon ± .05 mev	High Purity Si, obtained from Magneto-Phonon Resonance by Barres et al. 1975 ± .56	Comments
42.5 52.6	43.5 52.0	46.4 50.9	f phonons, strong in both Si:As and Si:P, they are a mixture of optical and acoustic motion.
60.4	60	60	f optical phonon, predicted to be very close to 60 mev. It is stronger in Si:P than Si:As.
65.5	65.0	65.9	either, or both, the g T.O. phonon at 65.3 mev and an intravalley T.O. phonon at a similar energy.
>55.5			A number of strong minima were observed, particu- larly at 65.1 and 63 mev. These could be fitted to combinations of the strongest phonons in the system, 2 phonons at 42.5 and 53.3 mev and 3 phonons enhanced phonons at 36.3 and 42.5 mev.
		72.7	A combination of the 60 mev phonon with a low energy g phonon.

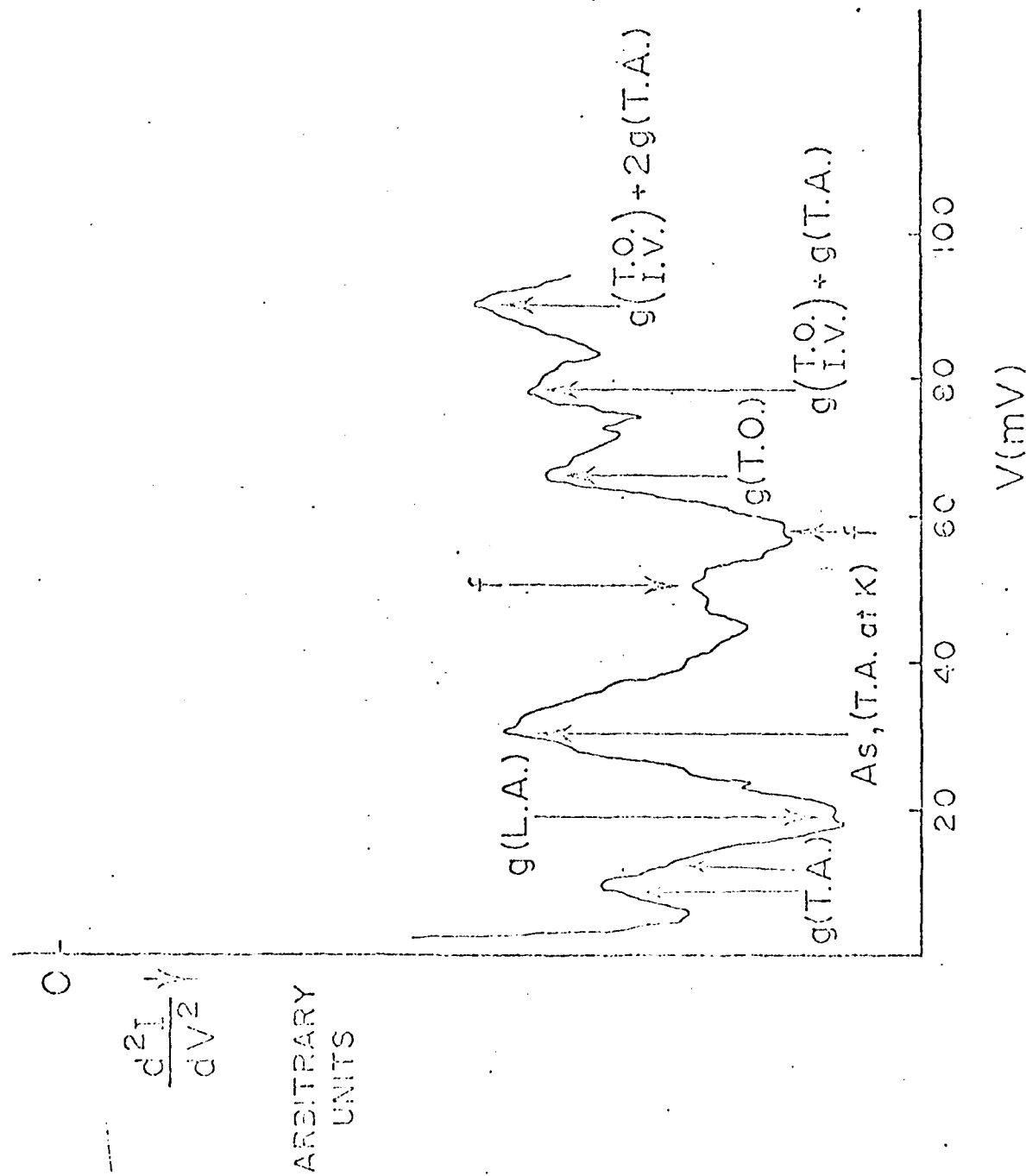
TABLE I contd.

Energy of phonon	Size of phonon	High Parity S1, obtained from Raman-scattering Ramanic 2 ² values c. 21. 1975 ± 3%	Comments
77.4			A combination of the 14.9 mev phonon and either the 21.0 or the 19.1 mev optical phonons.
22.7			A combination of the 21.2 mev Ramanic 2 ² and the 21.0 or 19.1 mev optical phonons.
≥30			A broad minimum with considerable structure due to combinations of optical phonons and the 30.5 mev mode.
320 mev			Two large minima separated by 6 mev, possibly conduction electron pair ion resonance.

INJECTION FROM AI INTO Si:As

Fig. 1

- 11 -



12

INJECTION INTO S.I.P., 4.2 K

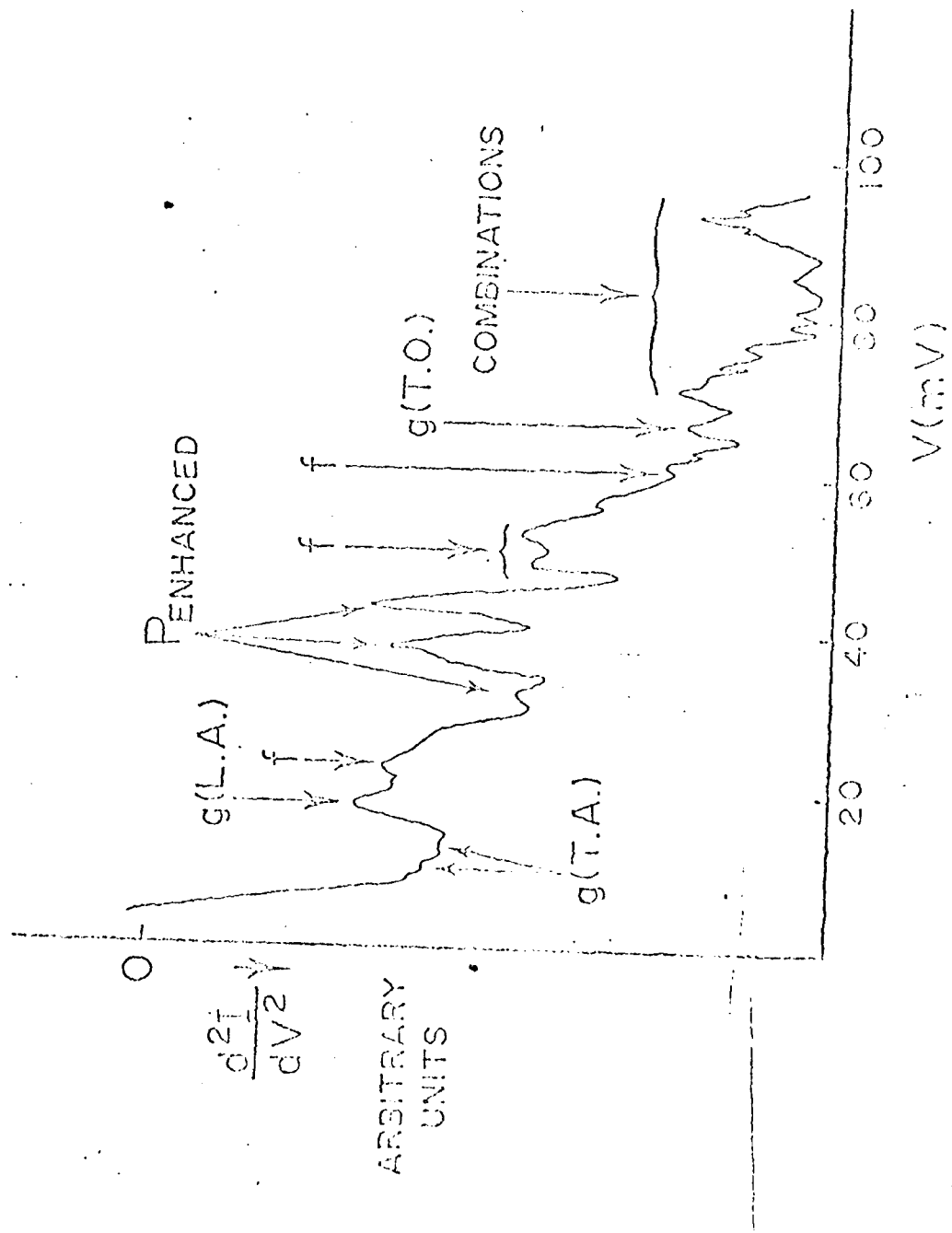


FIG. 3

INJECTION INTO Si:P

2.2 K

INJECTION INTO Al

QUANTUM EFFECTS?

$$\frac{d^2I}{dV^2}$$

PENHANCED MODES

$g(L.A.)$

$g(T.A.)$

V (mV)

40 20 0 20 40 60 80

22

SiAS

$$\frac{c^2}{c\sqrt{2}}$$

A

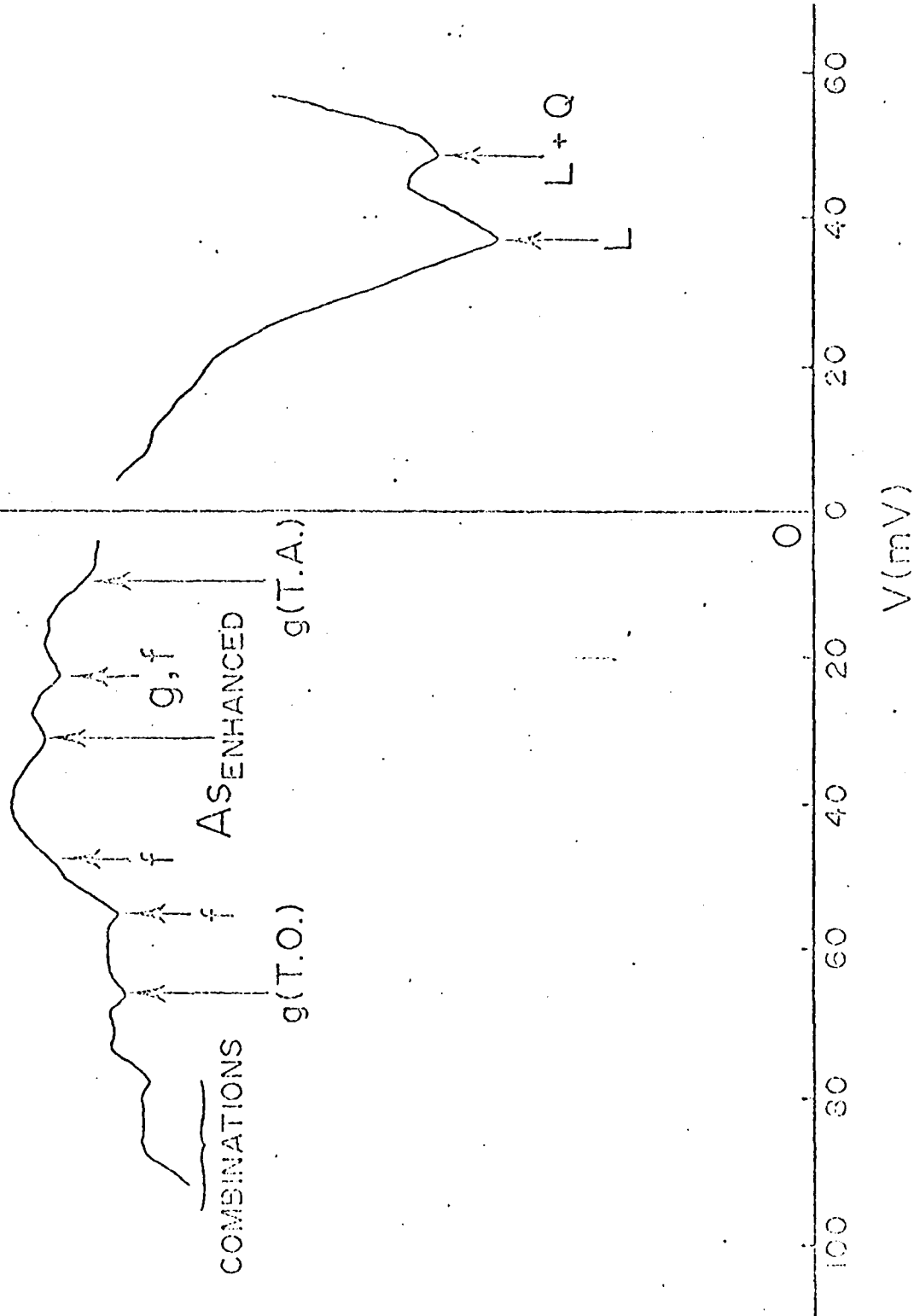
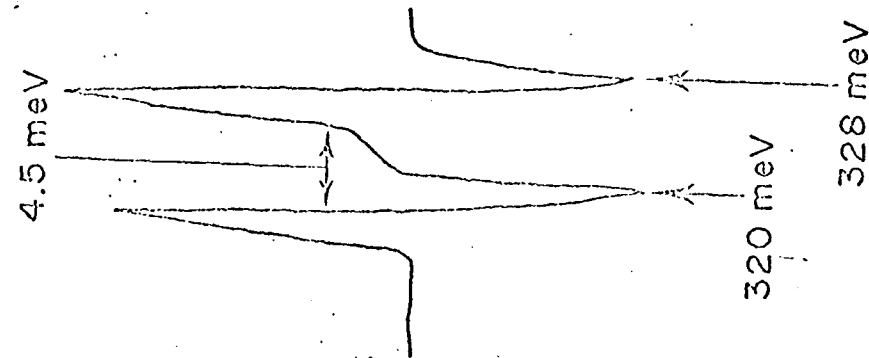


Fig. 5



1b Phonon spectroscopy of aluminium

In the previous section it was shown that electron injection into Si revealed the phonons responsible for scattering. When the $\Delta\ell$ is positive with respect to the Si, the d^2I/dV^2 against V plot shows minima corresponding to $\Delta\ell$ phonons, Figure 1. The clarity of this figure, and the generally clear observation of $\Delta\ell$ phonons, contrasts with the reported failure of $\Delta\ell$ - $\Delta\ell$ junctions¹.

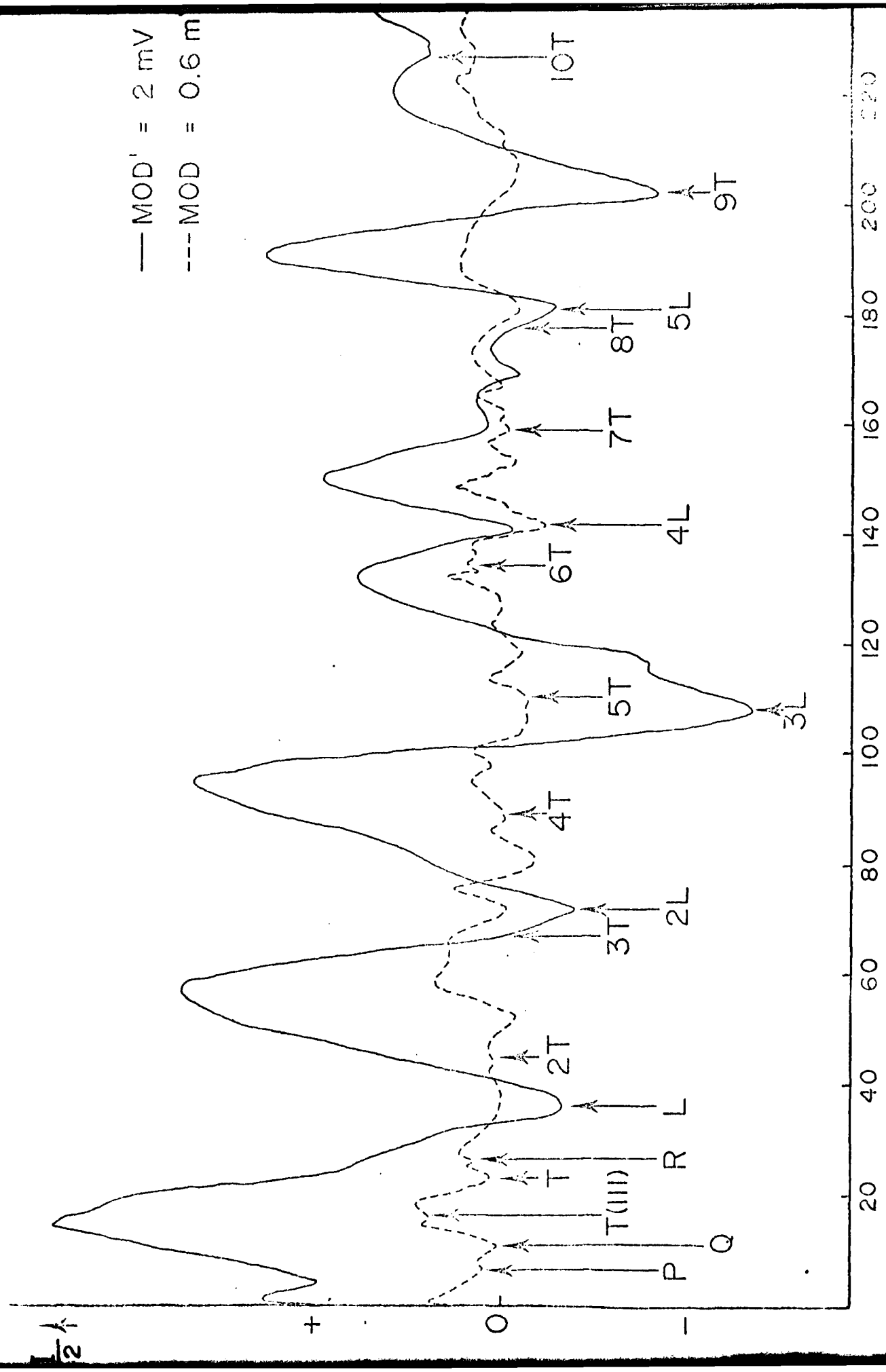
Inspection of the E-k diagram of $\Delta\ell$, (for example Harrison², shows that there are many possible types of phonon scattering. The most important processes are, a) between X points; b) between W points, ($W = \frac{1}{2}, 0, 1$); c) between U points, ($U = \frac{1}{4}, \frac{1}{2}, 1$); d) between X and W; e) between X and U; f) between W and U, and g) scattering between the two bands near U. The principal phonons involved in these processes have coordinates, a) (100) - an Umklapp process; b) (0, $\frac{1}{2}, \frac{1}{2}$) for both normal and Umklapp processes; c) (0, $\frac{1}{4}, \frac{3}{4}$); d) (0, 0, $\frac{1}{2}$), for normal and Umklapp processes; e) ($\frac{1}{4}, \frac{1}{4}, 0$) and ($\frac{1}{4}, \frac{3}{4}, 0$) for Umklapp processes; f) ($\frac{1}{4}, \frac{3}{4}, 0$), Umklapp process; g) this is a phonon close to the (100) direction, and, assuming only the component in this direction, has coordinates $\approx (0.17, 0, 0)$. From the $\Delta\ell$ phonon dispersion curves³, the phonons responsible are a) longitudinal, (L), and transverse, (T), phonons at the X point having energies of 37.5 meV and 22.5 meV; b) the (L) phonon with energy 35 meV, this phonon gives rise to the principal peak in the density of states. There are also two transverse phonons with the same momentum, T_1 at 19 meV and T_2 at 25 meV; c) the (L) phonon at the K point with energy 29 meV and two (T) phonons, T_1 , with a high density of states at 21 meV, and T_2 at 35 meV.

Thus scattering is accomplished principally by 35 meV L phonons and 21 - 22 meV T phonons. A range of phonons can cause processes d) - f), which will make identification difficult. On the other hand, process g) will be caused by low energy phonons and should be well defined. Inspection of the phonon dispersion curves shows that the possible phonon energies for process a) are, approximately, an L mode at 11 meV and a T mode at 6 meV. In Figure 1 these are identified as the minima P and Q at 6 meV and 12 meV respectively. Minimum R at 26 meV is identified as the T_2 phonon at ($\frac{1}{4}, \frac{1}{2}, 0$). A minimum found at 17 meV is attributed to the T phonon having coordinates (111), i.e. at the Γ point.

The major features of Figure 1 are clearly associated with the 35 meV L and 22 meV T phonons. In view of the many subsidiary minima, and the large number of possible phonon combinations, a detailed analysis of the figure was not performed. As seen in Figure 1, phonon combinations are clearly observed. It is not clear why combinations of L phonons fade out abruptly, or why the T combinations increase in strength above ≈ 160 meV. The degree of electron heating appears too small to sample additional features of the band structure. The combinations were observable for most of the specimens used in this work, except for that used for Figure 3 of the preceding section, where structure was not found past the principle L minimum.

The principle features of the $\Delta\ell$ observations were clear at 77 K, for example, the $\Delta\ell$ side of Figure 2 in the previous paper clearly shows the 35 meV L phonon, and, surprisingly, its combinations with the 12 meV Q phonon thought responsible for scattering near the U point.

Al SPECTRUM, 4.2 K



It is noteworthy that this experiment has revealed a clearer Al phonon spectrum than tunnelling experiments⁴. Possibly the Al filament is ordered by local heating during the formation process, or the electrons pass through the filament into the evaporated Al before being scattered back.

REFERENCES

- 1 Yansen, I.K., 1974 Soviet Phys. J.E.T.P., 39, 506
- 2 Harrison, W.A., 1966 Pseudopotentials in the Theory of Metals, Benjamin New York
- 3 Gilat, G. and Nicklow, R.M., 1966 Phys. Rev., 143, 487

FIGURE CAPTIONS

1. The plot of d^2I/dV^2 against V for injection into Al. The increase in low energy structure caused by decreasing the modulation voltage from 2mV (—) to 0.6 mV (---) is clear. The principal phonons and combinations are indicated and are discussed in the text. Sometimes those indicated were minima only at low modulation voltages, and shoulders at the higher modulation voltage. A wide range of combinations was found for a low modulation voltage. This was not analysed in detail.

1c Phonon and subband spectroscopy of silicon
inversion layers

For this work MOSFET's were fabricated on the (100) surface of $10 \Omega \text{ cm}$ p type Si, ($N_A = 2.10^{15} \text{ cm}^{-3}$). A filamentary contact was formed between the Al gate and the Si through 800 \AA of thermally grown SiO_2 . In order to sustain an inversion layer without applying a voltage to the gate, the SiO_2 was contaminated with Na^+ ions before evaporation of the Al. The Na^+ was drifted to the Si- SiO_2 interface, and the device was cooled to 77 K to freeze the Na^+ into position prior to formation of the filamentary contact. Unfortunately, at this temperature the resistance between the inversion layer and the substrate was too high, and the contact was always formed between the gate and the source or drain. The contact was formed satisfactorily at 300 K, but at this temperature some drift of the Na^+ occurred and the carrier concentration could not be defined more accurately than $2.5 \pm 0.5 \times 10^{12} \text{ cm}^{-2}$. Although the Si is p type, E_F at the Si surface is in the conduction band tail, and so a barrier does not exist between the Al and the inversion layer.

It was found that at 4.2 K the resistance of the inversion layer in series with the contact was too high for meaningful measurements to be taken. Consequently the experiment was performed at 77 K where

the resistance was considerably lower. A number of minima were found on the d^2I/dV^2 versus gate voltage plot for injection into the inversion layer; the principal L minimum was clearly observed for injection into the Al.

Before considering the phonon spectrum in the inversion layer, we first briefly discuss phonon scattering in this system. The inversion layer differs from bulk Si in that the degeneracy of the valleys is lifted by the strong surface field. For the (100) surface, the ground state, E_0 , is formed from the two valleys with heavy mass perpendicular to the interface; there is also a series of excited states associated with these two valleys, E_1 , E_2 , E_3 In addition, another ladder of energy levels is associated with the other four valleys which have light mass normal to the interface, E_0' , E_1' , E_2' Ando¹ has found that E_0' lies close to E_1 .

Intervalley scattering in the twofold degenerate levels is by g phonons. As there will be a sharp threshold for this process, it is observable despite the general background of intervalley scattering imposed by the absence of momentum conservation at the interface. For intrasubband transitions, the mobility is not affected by direct scattering along the major (100) axis. However, in systems with small k_F , phonons very close to the g energy will scatter effectively. As the energy of the injected electrons increases we would expect to observe g scattering in E_0 , followed by g scattering in E_1 , and both g and f scattering in E_0' as well as f scattering between E_0' and both E_0 and E_1 . Scattering between subbands formed from the same set of valleys is forbidden in the zeroth order². Scattering across the Fermi surface by long wavelength phonons will not be observed.

The minima in d^2I/dV^2 as a function of V were found and identified as particular phonons. However, two weak minima were found which could not be ascribed to phonons. If these were identified as the bottom of new subbands, a whole new phonon series followed in a rational way. These minima were at 29 meV and 55 meV. The energies are above the Si Fermi level, which cannot be ascertained directly due to a lack of precise knowledge of carrier concentration. Ignoring the existence of band tailing, and assuming a carrier concentration of $2.5 \pm 0.5 \times 10^{12}$, we find that E_F is roughly 12 meV. Thus the subbands are ~ 41 meV and ~ 67 meV above the bottom of E_0 . These energies appear too great for $|E_1 - E_0|$ and $|E_2 - E_0|$ for the value of substrate doping. In fact the phonon spectrum suggested that the subbands are E_0' and E_1' . This was not surprising as E_0 only gave one reasonable minimum - the 65 meV g phonon. The details of E_1 and E_2 appear lost in the complex spectra of E_0' and E_1' . The cause of the observation of weak minima corresponding to the onset of subbands must be in the greater density of states enhancing the probability of backscattering by phonon absorption. A very weak minimum was identified at ~ 7 meV, possibly this is due to surface (Rayleigh) phonons which may be important in determining the low temperature mobility.

Turning now to the detailed results shown in Table 1. It was barely possible to identify the low energy g phonons although the 65 meV g phonon was clear. A minima was also observed at ~ 60 meV corresponding to an f phonon. This could not arise from scattering within the E_0 band, but from electrons injected into E_0' or E_1' being scattered into E_0 .

TABLE I
PRINCIPAL PHONONS PARTICIPATING IN INVERSION LAYER SCATTERING, 77K

	Energy of centre of minimum, meV \pm 1.0 meV	Energy above bottom of subband, meV \pm 1.0 meV	Identification
a) Ground Subband, E_0	7 13 18 60 63	7 13 18 60 63	Possible surface mode \int Extremely weak g phonons f phonon scattering electrons into this subband from another subband g or possibly intravalley phonon
b) Subband at 22 meV E_0'	33 40 47 52 78 90 96	9 11 18 24 49 61 67	\int g phonons g phonon f phonon f phonon, merged with an f phonon of the following series f phonon g or possibly intravalley phonon

TABLE I

contd.

	Energy of Centre of minimum, mev	Energy above bottom of subband, mev	Identification
c) Subband at 55 mev, E_1	66 77 78 105 103 115 122	11 22 23 50 53 60 67	Very broad g phonon g f, possibly merged with an f phonon of preceding series Appeared to be two partially resolved f phonons f phonon g or possibly intravalley phonon

Examination of the phonon series for the subband starting at 29 meV shows generally clear evidence of f scattering, supporting identification as E'_1 . The electrons participating in this process may be scattered within E'_1 , or into this subband from E_0 .

The subband commencing at 55 meV displays a comprehensive phonon spectrum, but it cannot be directly ascertained if this is of the E or E' series. The existence of f scattering is not conclusive as, in the absence of compression experiments, it cannot be determined if this is inter or intrasubband scattering. However, the strength of the g minimum is more akin to E'_0 than E_0 , and so we tentatively identify this subband as E' .

Further minima were observed at 128, 133 and 140 meV, and considerable structure was found at energies greater than 120 meV. Due to the complexity of identification, further analysis was not performed. These minima may result from higher subbands, phonon combinations or possibly plasmons.

In conclusion, this appears to be a promising technique for the investigation of both phonon scattering, which can be clarified by the application of compression, plasmon effects and subband spectroscopy. In this latter context, it is to be noted that it is possible to vary the subband splitting by the application of substrate bias.

REFERENCES

- 1 Ando, T., 1978 Surface Science, 73, 1
- 2 Ferry, D.K., 1975 Surface Science, 57, 218

2. A new method for high accuracy determination of the fine structure constant based on quantized Hall resistance*

In this section we report a new, potentially high-accuracy method for determining the fine-structure constant, α . The new approach is based on the fact that the degenerate electron gas in the inversion layer of a MOSFET (metal-oxide-semi-conductor field-effect transistor) is fully quantized when the transistor is operated at helium temperatures and in a strong magnetic field of order 15 T^1 . The electric field perpendicular to the surface (gate field) produces subbands for the motion normal to the semiconductor-oxide interface, and the magnetic field produces Landau quantization of motion parallel to the interface. The density of states $D(E)$ consists of broadened δ functions²; minimal overlap is achieved if the magnetic field is sufficiently high. The number of states, N_L , within each Landau level is given by

$$N_L = eB/h, \quad (1)$$

*Experiments performed by K. von Klitzing of Wurzburg University, West Germany, as part of a collaborative project.

where we exclude the spin and valley degeneracies. If the density of the states at the Fermi energy, $N(E_F)$, is zero, an inversion layer carrier cannot be scattered, and the centre of the cyclotron orbit drifts in the direction perpendicular to the electric and magnetic field. If $N(E_F)$ is finite but small, an arbitrarily small rate of scattering cannot occur and localization produced by the long lifetime is the same as a zero scattering rate, i.e., the same absence of current-carrying states occurs³. Thus, when the Fermi level is between Landau levels the device current is thermally activated and the minima in σ_{xx} , σ_{xx}^{\min} , can be less than $10^{-7}\sigma_{xx}^{\max}$ ⁴. Increasing the magnetic field and decreasing the temperature, further decreases σ_{xx}^{\min} . The Hall conductivity σ_{xy} , which is usually a complicated function of the scattering process, becomes very simple in the absence of scattering and is given by²

$$\sigma_{xy} = -Ne/B \quad (2)$$

where N is the carrier concentration.

The correction term to the above relation, $\Delta\sigma_{xy}$, is of the order of $\sigma_{xx}/\omega\tau$, where ω is the cyclotron frequency and τ is the relaxation time of the conduction electrons; $\omega\tau \gg 1$ in strong magnetic fields. When the Fermi energy is between Landau levels, and $\sigma_{xx}^{\min} \sim 10^{-7}\sigma_{xx}^{\max}$, the correction $\Delta\sigma_{xy}/\sigma_{xy} < 10^{-8}$. Subject to any error imposed by $\Delta\sigma_{xy}$, when a Landau level is fully occupied and $N = N_{Li}$ ($i = 1, 2, 3 \dots$), σ_{xy} is immediately given from equations (1) and (2):

$$-\sigma_{xy} = e^2 i/h. \quad (3)$$

The Hall resistivity $\rho_{xy} = -\sigma_{xy}/(\sigma_{xx}^2 + \sigma_{xy}^2) = -\sigma_{xy}^{-1}$ is defined by E_H/j (E_H = Hall field, j = current density) and can be rewritten R_H/I , where R_H is the Hall resistance, U_H the Hall voltage and I the current. Thus, $R_H = h/e^2 i$, which may finally be written as⁵

$$R_H = \alpha^{-1} \mu_0 c / 2i, \quad (4)$$

where μ_0 is the permeability of vacuum and exactly equal to $4\pi \times 10^{-7} \text{ H m}^{-1}$, c is the speed of light in vacuum and equal to $299\ 792\ 458 \text{ m s}^{-1}$ with a current uncertainty of 0.004 ppm and $\alpha = \frac{1}{137}$ is the fine-

structure constant. It is clear from equation (4) that a high-accuracy measurement of the Hall resistance in SI units to a few parts in 10^3 by means of the so-called calculable cross capacitor by Thompson and Lampard⁶, the question of absolute units versus as-maintained units is much less of a problem than in the determination of e/h from the ac Josephson effect. Furthermore, the magnitude of R_H falls within a relatively convenient range: $R_H \approx (25\ 813 \Omega)/i$, with i typically between 2 and 8. Finally, we note that if α is assumed to be known from some other experiment (for example, from $2e/h$ and the proton gyromagnetic ratio γ_p), equation (4) may be used to derive a known standard resistance.

Two well-known corrections in the low-field Hall effect become unimportant. The first is the correction due to the shorting of the Hall voltage by the source and drain contacts⁷. This is important at low fields for samples with length-to-width ratio, L/W , less than 4, but becomes negligible when the Hall angle is 90° , i.e., $\sigma_{xx} = 0$.⁸ The second correction which becomes unimportant is that due to an

inexact alignment of the Hall probes, i.e., they are not exactly opposite. This is irrelevant, as the voltage drop along the sample vanishes when $\sigma_{xx} = 0$.⁹

The experiments were carried out on MOS devices with a range of oxide thicknesses ($d_{ox} = 100$ nm - 400 nm), and length-to-width ratios ranging from $L/W = 25$ to $L/W = 0.65$. All the transistors were fabricated on the (100) surface orientation and, typically, the p-type substrate had room temperature resistivity of $10 \Omega \text{ cm}$. The resistivity at helium temperature was higher than $10^{13} \Omega \text{ cm}$, and no current flow between source and drain around the channel could be measured. The long devices ($L/W > 8$) had potential probes in addition to the Hall probes.

The measured voltage U_{pp} is proportional to the resistivity component $\rho_{xx} = \sigma_{xx}[\rho_{xx}^2 + \rho_{xy}^2]$. At gate voltages where the E_F is in the energy gap between Landau levels, minima in both σ_{xy} and ρ_{xx} are observed⁹. Such minima are clearly visible, and are identified, in Figure 1; the minima due to the lifting of the spin and the (twofold) valley degeneracy are also apparent. The Hall voltage clearly levels off at these values of carrier concentration where σ_{xy} and ρ_{xx} are zero. The values of U_H obtained in the regions are in good agreement with the predicted values, equation (4), if the error due to the 1-MΩ input impedance of the X-Y recorder is taken into account. It was found that the value of U_H in the "steps" was, for constant current, independent of sample geometry and direction of magnetic field, provided that σ_{xx} was zero.

An area of possible criticism of the theoretical basis of this experiment is the role of carriers which are localized outside the main Landau level. Here we do not specify the localization mechanism, but the presence of localized carriers will invalidate both the relation $N = N_L$ and equation (4). However, the experimental results strongly suggest that such carriers do not invalidate equation (4). At present there is both theoretical and experimental investigation of this type of localization^{3, 4, 9-12}. Ando² has suggested that the electrons in impurity bands, arising from short range scatterers, do not contribute to the Hall current; whereas the electrons in the Landau level give rise to the same Hall current as that obtained when all the electrons are in the level and can move freely. Clearly this process must be carefully examined as an accompaniment to highly accurate measurements of Hall resistance.

For high-precision measurements we used a normal resistance R_0 in series with the device. The voltage drop, U_0 , across R_0 , and the voltages U_H and U_{pp} across and along the device was measured with a high impedance voltmeter ($R > 2 \times 10^{10} \Omega$). The resistance R_0 was calibrated by the Physikalisch Technische Bundesanstalt, Braunschweig, and had a value of $R_0 = 9929.69 \Omega$ at a temperature of 20°C . A typical result of the measured Hall resistance $R_H = U_H/I = U_{H0}R_0/U_0$, and the resistance, $R_{pp} = U_{pp}R_0/U_0$, between the potential probes of the device is shown in Figure 2 ($B = 13$ T, $T = 1.3$ K). The minimum in σ_{yy} at $V_g = 23.6$ V corresponds to the minimum at $V_g = 8.7$ in Figure 1, because the thicknesses of the gate oxides of these two samples differ by a factor of 3.6. Our experimental arrangement was not sensitive enough to measure a value of R_{pp} of less than 0.1Ω ; it was found in the gate-voltage region $23.40 \leq V_g \leq 23.60$. The Hall resistance in this gate voltage region had a value of $6753.3 \pm 0.1 \Omega$. This inaccuracy of

$\pm 0.1 \Omega$ was due to the limited sensitivity of the voltmeter. We would like to mention that most of the samples, especially devices with a small length-to-width ratio, showed a minimum in the Hall voltage as a function of V_g at gate voltages close to the left side of the plateau. In Figure 2, this minimum is relatively shallow and has a value of 6452.87Ω at $V_g = 23.30$.

In order to demonstrate the insensitivity of the Hall resistance on the geometry of the device, measurements on two samples with a length-to-width ratio of $L/W = 0.65$ and $L/W = 25$, respectively, are plotted in Figure 3. The gate-voltage scale is given in arbitrary units, and is different for the two samples because the thicknesses of the gate oxides are different. A gate voltage $V_g = 1.00$ corresponds, approximately, to a surface carrier concentration where the first fourfold-degenerate Landau level, $n = 0$, is completely filled. Within the experimental accuracy of 0.1Ω , the same value for the plateau in the Hall resistance is measured. The value for $h/4e^2 = 6453.201 \pm 0.005 \Omega$ based on the recommended value for the fine-structure constant⁵ is plotted in this figure, too. The decrease of the Hall resistance with decreasing gate voltage for the sample with $L/W = 0.65$ originates mainly from the shorting of the Hall voltage at the contacts. This effect is most pronounced when the Hall angle becomes smaller than 90° . In the limit of small Hall angles, the Hall voltage is reduced by a factor of 2 for the sample with $L/W = 0.65$.⁷

The mean value of the Hall resistance for all samples investigated was $6453.22 \pm 0.10 \Omega$ for measurements in the energy gap between the Landau levels $n = 0$ and $n = 1$ (corresponding to $i = 4$ in equation 4), $3226.62 \pm 0.10 \Omega$ for measurements in the energy gap between Landau levels $n = 1$ and $n = 2$ ($i = 8$), and $12\ 906.5 \pm 1.0 \Omega$ for measurements in the energy gap between the spin split levels with $n = 0$ ($i = 2$). These resistances agree very well with the calculated values of $h/e^2 i$ based on the recently reported¹³ highly accurate value of $a^{-1} = 137.035\ 963(15)$ (0.11 ppm).

Measurements with a voltmeter with higher resolution and a calibrated standard resistor with a vanishing small temperature coefficient at $T = 25^\circ\text{C}$ yield a value of $h/4e^2 = 6453.17 \pm 0.02 \Omega$ corresponding to a fine-structure constant of $a^{-1} = 137.0553 \pm 0.0004$.

REFERENCES

- 1 For a review see for example: F. Stern, Crit. Rev. Solid State Sci., 5, 499 (1974); G. Landwehr, in Advances in Solid State Physics: Festkörperprobleme, ed. H.J. Queisser (Pergamon) 15, 48 (1975)
- 2 Ando, T., 1974 J. Phys. Soc. Jpn., 37, 622
- 3 Acki, H. and Karimura, H., 1977 Solid State Comm., 21, 45
- 4 Nicholas, J.J., Stadling, R.A. and Tidley, R.J., 1977 Solid State Comm., 21, 341
- 5 Cohen, E.R. and Taylor, E.H., 1973 J. Phys. Chem. Ref. Data, 2, 633
- 6 Thompson, A.M. and Lonsdale, D.G., 1976 Nature (London), 277, 883
- 7 Isenberg, I., Jarrell, P.H. and Greene, P.R., 1948 Rev. Sci. Instrum., 19, 773
- 8 Wick, R.F., 1951 J. Appl. Phys., 22, 741

9 Englert, Th. and Klitzing, K.V., 1978 Surf. Sci., 73, 71
10 Kawaji, S. and Wakabayashi, J., 1976 Surf. Sci., 59, 238
11 Pepper, M., 1978 Philos. Mag., 37B, 83
12 Kawaji, S., 1978 Surf. Sci., 73, 46
13 Williams, E.R. and Olsen, P.T., 1979 Phys. Rev. Lett., 42, 1575

FIGURE CAPTIONS

1. Recordings of the Hall voltage U_{HJ} , and the voltage drop between the potential probes, U_{pp} , as a function of the gate voltage V_g at $T = 1.5$ K. The constant magnetic field (B) is 18 T and the source drain current, I , is 1 μ A. The inset shows a top view of the device with a length of $L = 100 \mu\text{m}$, a width of $W = 50 \mu\text{m}$, and a distance between the potential probes of $L_{pp} = 130 \mu\text{m}$.
2. Hall resistance R_H , and device resistance, R_{pp} , between the potential probes as a function of the gate voltage V_g in a region of gate voltage corresponding to a fully occupied, lowest ($n = 0$) Landau level. The plateau in R_H has a value of $6453.3 \pm 0.1 \Omega$. The geometry of the device was $L = 400 \mu\text{m}$, $W = 50 \mu\text{m}$, and $L_{pp} = 130 \mu\text{m}$; $B = 13$ T.
3. Hall resistance R_H for two samples with different geometry in a gate-voltage region V_g where the $n = 0$ Landau level is fully occupied. The recommended value $h/4e^2$ is given as 6453.204Ω .

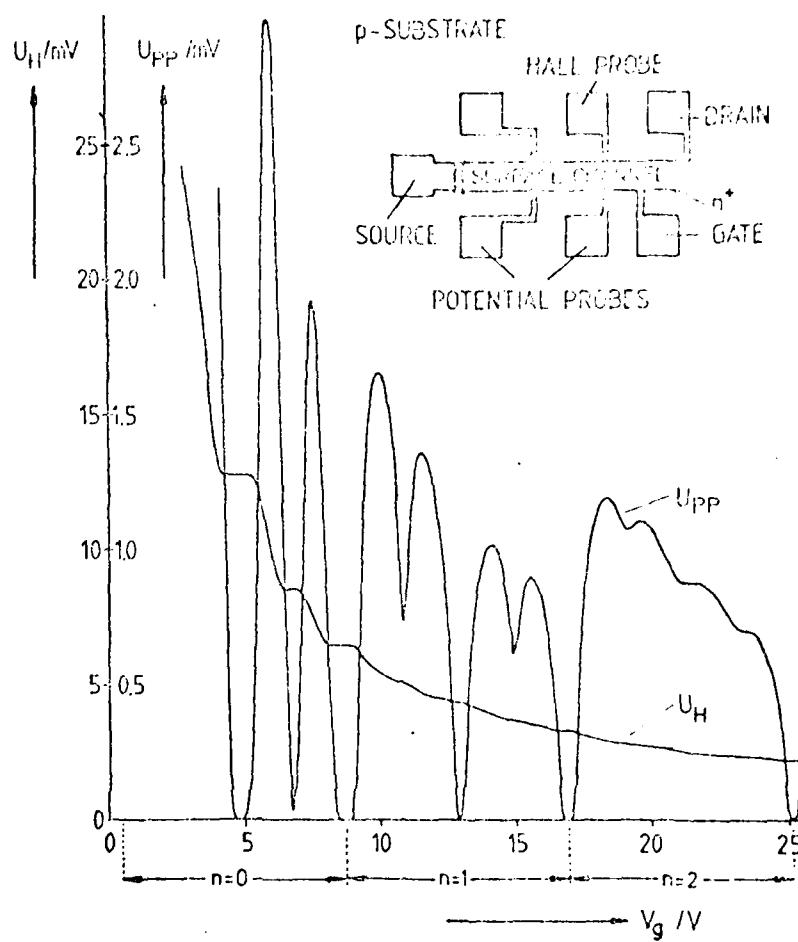


FIGURE 1.

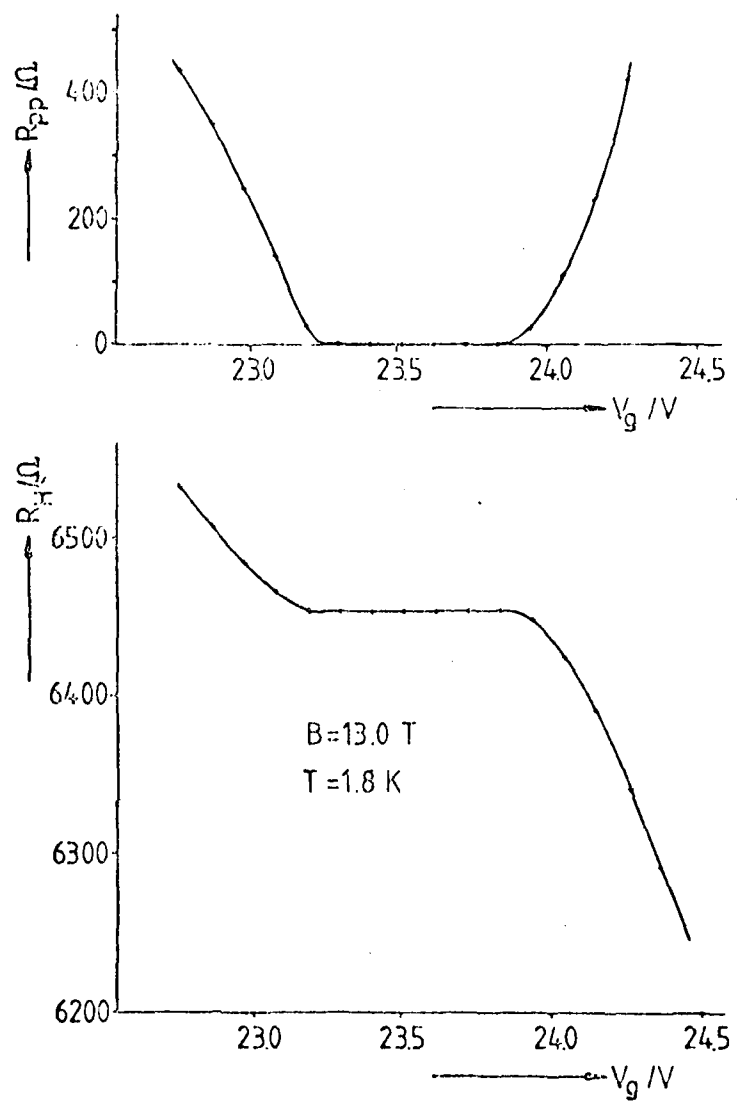


FIGURE 2.

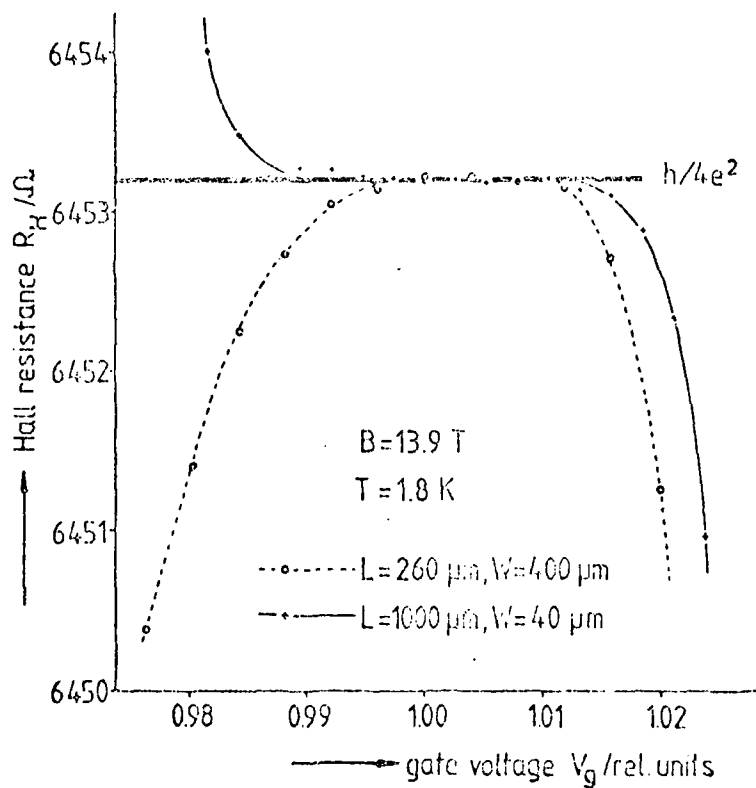


FIGURE 3.

